Automotive Science and Engineering, Vol. 14, No. 2, (2024), 4353-4359

Iran University of Science and Technology

Automotive Science and Engineering

Journal Homepage: ase.iust.ac.ir

ISSN: 2008-9899

Improving energy harvesting in automotive applications: comparative analysis of ZnO Nanostructures for flexible piezoelectric devices

Seied Isa Koranian [1*], Mahdi Gholampour [1], Hamid Mazandarani[2]

[1] Physics Group, Faculty of Basic Science, Imam Ali University, Tehran, Iran.

[2] Physics Department, Iran University of Science and Technology, Tehran, Iran.

ARTICLE INFO

Article history:

Received : 5 Jan 2024

Accepted: 25 Mar 2024

Published: 6 Apr 2024

Keywords:

smart vehicles

nanogenerator

energy harvesting

piezoelectric effect

ZnO nanostructure

A B S T R A C T

Fueled by their potential for energy harvesting, ZnO nanorods (NRs) have sparked considerable enthusiasm in the development of piezoelectric nanogenerators in the last decade. This is attributed to their exceptional piezoelectric properties, semiconducting nature, cost-effectiveness, abundance, chemical stability in the presence of air, and, the availability of diverse and straightforward crystal growth technologies. This study explores and compares the piezoelectric properties of two promising nanostructured ZnO architectures: thin films deposited via radiofrequency (RF) magnetron sputtering and well-aligned nanorod arrays grown using a hydrothermal process. Both structures are fabricated on flexible polyethylene terephthalate (PET) with an indium tin oxide (ITO) electrode (PET-ITO substrate), presenting valuable options for flexible piezoelectric devices. By directly comparing these distinct morphologies, we provide insights into their respective advantages and limitations for energy harvesting and sensor applications. The investigation into the piezoelectric properties of ZnO NRs involved the construction of an actual piezoelectric nanogenerator. This device demonstrated a direct correlation between applied mechanical forces and the resultant voltage outputs. It was observed that when the same external force was applied to both devices, the ZnO NRs-based piezoelectric nanogenerator (PENG) exhibited a higher output voltage compared to the other device.

1. Introduction

Driven by the twin threats of declining fossil fuel reserves and the escalating crisis of carbon dioxide emissions, the contemporary era urgently demands the investigation and advancement of clean and renewable energy sources [1]. Leveraging the inherent advantages of nanostructured materials, researchers are actively exploring various strategies for environmental energy harvesting within the field of nanotechnology [1]. The emerging domain of PENGs presents an innovative approach to harnessing various forms of mechanical energy, including movements of the human body, wind, tidal forces, or vibrations [2]. These devices operate based on the intrinsic capability of nanostructured piezoelectric materials to produce electrical potentials when subjected to mechanical deformation [2]. When effectively utilized within a closed circuit, this phenomenon facilitates ongoing electricity generation as long as the mechanical stimuli persist [2]. PENGs hold immense potential for a variety of applications within the smart vehicle and automotive industry, thanks to their ability to harvest energy from readily available sources like vibrations, pressure changes, and even wind. Here are some exciting possibilities: (a) Tire pressure monitoring: Integrated into tires, PNGs could generate electricity from the deformation caused by rolling,

*Corresponding Author
Email : Seiedisa.koranian@gmail.com
https://doi.org/10.22068/ase.2024.664

"*Automotive Science and Engineering*" is licensed under a Creative Commons Attribution-Noncommercial 4.0 International License.

[Downloaded from azadandishi.iust.ac.ir on 2025-07-21]

[DOI: 10.22068/ase.2024.664]

powering wireless tire pressure sensors and eliminating the need for battery replacements [3–5]. (b) Suspension systems: PNGs in shock absorbers could convert suspension movement into electricity, powering onboard sensors for monitoring road conditions and vehicle health [3–5]. (c) Aerodynamic elements: Wind flowing over spoilers or other aerodynamic components could be harvested by PNGs to power sensors for active control systems or even small electronics like LED brake lights [3–5]. Zinc oxide (ZnO) rises to the forefront as a promising material for piezoelectric applications due to its unique combination of properties [6]. This wide bandgap semiconductor boasts several advantages, including its abundance in nature, affordability, inherent stability in air, and biocompatibility [6]. Crucially, ZnO exhibits a crystal structure (hexagonal wurtzite) that lacks a center of symmetry under normal conditions [6]. This asymmetry, created by the arrangement of Zn^{2+} and O^{2-} ions, grants ZnO its intriguing piezoelectric property. Imagine applying pressure to the tip of a tetrahedron representing ZnO's structure [7]. This pressure disrupts the perfect balance between positive and negative charges, generating a net polarization and surface charges. This phenomenon lies at the heart of ZnO's piezoelectricity [7]. When mechanical stress is applied, the individual dipoles within the ZnO crystal align, creating an internal electric field [7]. This field manifests as a measurable voltage (piezo-potential) across the material's opposite faces. The remarkable feature of ZnO is its ability to convert this mechanical energy into electrical energy. As long as the stress persists, continuous piezo-charges and a piezo-potential are generated, driving a flow of electrical charges within the crystal towards an external circuit [7]. Essentially, ZnO acts as a tiny power generator, harnessing the energy from mechanical motion and transforming it into usable electricity [6, 8]. This study delves into the exciting potential of ZnO nanomaterials for energy harvesting by comparing two nanogenerator designs: one utilizing a thin film and another employing nanorods. Notably, the nanorod-based device exhibited far superior piezoelectric performance, highlighting the distinct advantages of this nanostructure for efficient energy conversion.

2. Materials and Method

The experimental section comprises two distinct segments: (a) the deposition of the ZnO thin film on the PET-ITO substrate using RF sputtering magnetron, and (b) the vertical growth of well-aligned the ZnO nanorods on the substrate through a hydrothermal process.

2.1. Deposition of a thin ZnO film on PET-ITO substrate

A 300 nm ZnO thin film was deposited on flexible PET-ITO substrate using magnetron sputtering at ambient temperature. The process employed an output power of 80 W, starting at a base pressure of 1×10^{-5} mTorr and reaching a deposition pressure of 8 mTorr. Crucially, the substrate requires meticulous cleaning prior to ZnO thin film deposition.

2.2. vertically growth of well-aligned ZnO NRs arrays

To ensure pristine surfaces for growth, the substrates underwent a rigorous cleaning process. Initially, they were immersed in a mixture of ethanol and distilled water within an ultrasonic bath, leveraging the cavitation effects to dislodge contaminants. Subsequently, the substrates were oven-dried to completely remove any residual moisture, which could hinder subsequent film deposition. Prior to growth of the well-aligned ZnO NRs, a crucial step involved depositing a seed layer onto the meticulously cleaned substrates. This seed layer, prepared by dissolving zinc acetate dehydrate in ethanol and Triethylamine, was applied using a spin coating system at 3000 rpm for 30 seconds to ensure a uniform and adherent layer. Subsequently, the coated substrates were oven-dried at 70°C for one hour to remove any residual solvent and promote subsequent growth. The synthesis of ZnO NRs employed a hydrothermal technique following the seed layer deposition. An aqueous growth solution was prepared by dissolving equimolar amounts (10 mM) of zinc nitrate hexahydrate and hexamethylenetetramine (HMTA) in 100 ml of deionized (DI) water. This solution was then transferred to a sealed stainless-steel autoclave lined with Teflon, where the pre-seeded substrate was carefully placed in a horizontal orientation. The autoclave was heated about 85°C in an oven for 4 hours. Once the growth process was complete, the substrate was retrieved from the solution, meticulously washed with DI water to remove any residual precursors, and finally air-dried for further use.

3. Results and Discussion

3.1. X-Ray Diffraction (XRD) analysis

X-ray diffraction (XRD) analysis (Figure 1(a), and 1(b)) reveals the crystalline structure of both the ZnO nanorods and thin film. Matching the observed diffraction peaks with standard JCPDS

[Downloaded from azadandishi.iust.ac.ir on 2025-07-21]

[DOI: 10.22068/ase.2024.664]

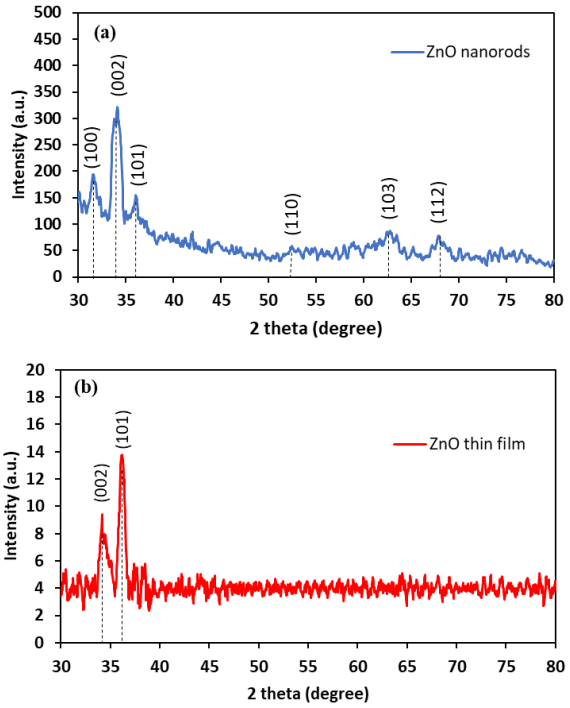

Figure 1: XRD pattern of the (a) ZnO nanorods, and (b) ZnO thin film.

reference patterns (No. 75-1526 and 36-1451) conclusively confirms the presence of the hexagonal wurtzite phase in both samples [9, 10]. The XRD pattern in Figure 1(a) exhibits a dominant (002) peak with significant intensity compared to other peaks like (101) and (100). This signifies preferential growth of the ZnO nanorods along their polar planes, particularly the c-axis (perpendicular to the substrate) [9, 10].

In the context of the Debye-Scherrer formula (1), the symbol θ refers to the Bragg diffraction angle measured in degrees, λ represents the utilized X-ray wavelength (fixed at 1.5406 Å), and β corresponds to the full-width at half maximum (FWHM) of the analyzed diffraction peak, expressed in radians. These parameters are then used to estimate the average crystalline size of the investigated material [9, 10]:

$$D = 0.9\lambda/\beta cos\theta \quad (1)$$

The key parameters extracted from XRD analysis, including FWHM and average crystalline size, are presented in Table 1 for both the ZnO thin film and ZnO nanorods.

3.2. Fourier-transform infrared (FTIR) spectroscopy

FTIR characterization was utilized to further investigate the structural features of the ZnO nanostructure, as illustrated in Figure 2 [11].

Table 1: FWHM and average crystalline size of the ZnO thin film and ZnO nanorods

Nanostructure	$FWHM_{(002)}$ (Degree)	Average crystalline size (nm)
ZnO thin film	0.99	8.5
ZnO nanorods	1.19	6.98

The transmittance spectra of both the ZnO thin film and nanorods revealed distinct peaks, corroborating the wurtzite structure observed in the XRD analysis. Characteristic absorption bands below 1000 cm^{-1} are often observed in the FTIR spectra of metal oxides, arising from vibrations within their crystal lattices. FTIR results revealed distinct absorption peaks around 470-600 cm^{-1}, corresponding to Zn-O stretching vibrations and corroborating the ZnO structure. FTIR spectra revealed peaks at 1380.84 and 1450.21 cm^{-1}, corresponding to C–O stretching vibrations. This observation directly implicates the use of zinc acetate as a precursor in the reaction, as these functionalities are characteristic of its structure. The presence of a peak at 1600-1700 cm^{-1} confirms the existence of C=O stretching vibrations. A peek at the spectrum reveals two telltale signs: peaks at 2900 cm^{-1} and 3300 cm^{-1}. These signatures point to the presence of C-H and OH groups in the sample, with the first peak arising from the stretching of C-H bonds and the second from the stretching of OH bonds [11–13].

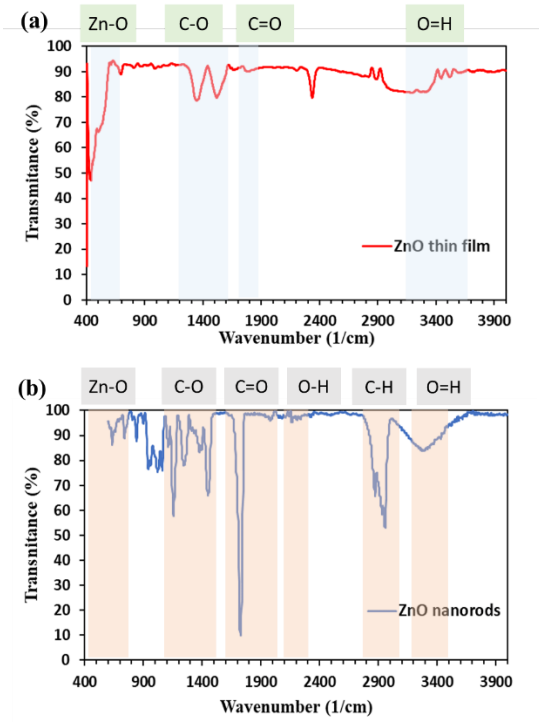

Figure 2: The FTIR spectrum of the (a) ZnO thin film (b) ZnO nanorods

[Downloaded from azadandishi.iust.ac.ir on 2025-07-21]

[DOI: 10.22068/ase.2024.664]

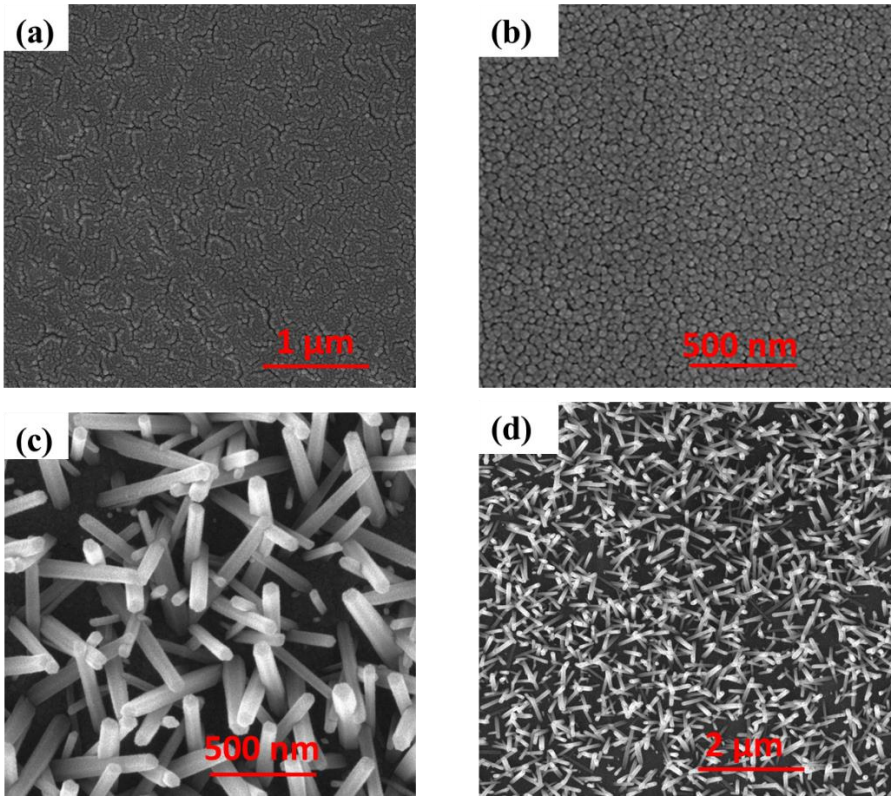

Figure 3: Top view SEM image of (a) bare PET-ITO substrate (b) the ZnO thin film (c) and (d) well-aligned ZnO nanorods arrays with 500 nm and 2 µm, respectively.

3.3. Scanning electron microscopy (SEM)

The SEM depiction of the PET-ITO substrate prior to ZnO nanorod growth is presented in Figure 3(a), providing a clear view of the substrate's morphology. Figure 3(b) presents SEM images, detailing the structural characteristics of the ZnO thin film. Figure 3(b) reveals the exceptional quality of ZnO thin films achieved using this single-step coating process. The film demonstrates remarkable uniformity, dense packing, and a fine-grained structure with an average grain size of approximately 50 nm. Well-aligned ZnO nanorods arrays with an average length of ~650 nm and a diameter ranging from 50 to 70 nm are visualized in the SEM image of Figure 3(c) and 3(d) with 500 nm and 2 µm magnitude, respectively. As illustrated in Figure 3(c) and 3(d), densely packed and strikingly uniform ZnO nanorods grow vertically on the substrate, forming a highly ordered arrangement which is in good agreement with the XRD results (Figure 1(b)).

3.4. Piezoelectric characterization

Figure 4 illustrates the voltage generated by the prepared piezoelectric nanogenerator. Both the ZnO thin film and nanorods, upon experiencing an external vibrational mechanical force, deform and create an electrical potential difference due to their inherent piezoelectric properties. This potential difference drives the observed current flow. The results clearly indicate that the output voltage generated by the piezoelectric nanogenerator (PENG) employing ZnO nanorods, approximately 0.68 mV, markedly exceeded that of the PENG relying on ZnO thin film, which registered at approximately 0.18 mV. Compared to thin films, nanorods boast several compelling advantages, making them a promising nanostructure for piezoelectric applications: Firstly, nanorods synthesis shines through its simplicity and affordability. Wet chemical methods, operable at surprisingly low temperatures (below 100 °C), can produce them on diverse substrates of any shape. This contrasts with the complex and often expensive high-temperature techniques needed for high-quality thin films. Secondly, nanorods are champions of flexibility. Their slenderness and minuscule diameter grant them remarkable softness, allowing them to bend and twist extensively (up to 6% under strain) without breaking, unlike thin films which crack easily under minimal stress. Thirdly, nanorods boast exceptional durability. Their small size translates to incredible structural strength, making them

[Downloaded from azadandishi.iust.ac.ir on 2025-07-21]

[DOI: 10.22068/ase.2024.664]

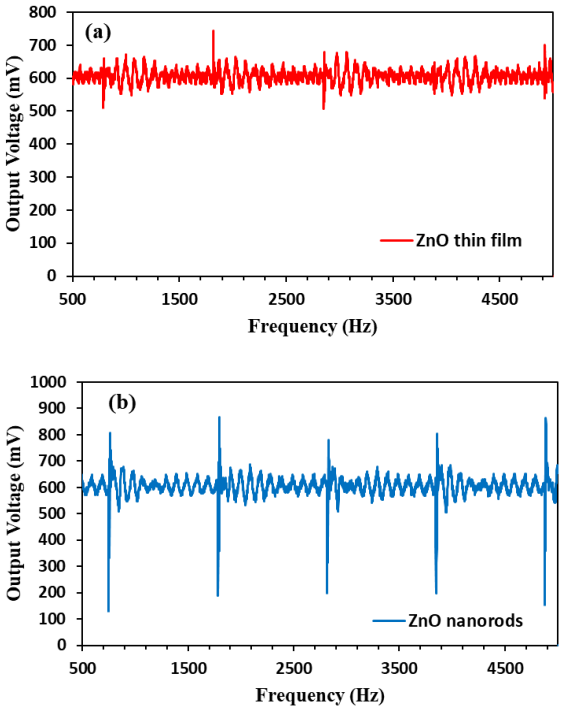

Figure 4: Voltage outputs generated from PENG based on the (a) ZnO thin film (b) ZnO nanorods

highly resistant to fatigue and wear. Thin films, on the other hand, are more susceptible to damage over time. Fourthly, even the faintest touch can stir nanowires into action. This remarkable sensitivity to external forces makes them ideal candidates for ultrasensitive devices capable of detecting minute changes. Finally, nanowires have the potential to pack a bigger piezoelectric punch. Compared to thin films, they might exhibit a higher piezoelectric coefficient, allowing them to convert mechanical energy into electricity more efficiently [7, 14, 15].

Crucially, the substrate's resistance, measured at 17 ohms using a four-point probe, enables us to determine the output current with Ohm's Law (I = V/R). Table 2 summarizes the calculated output voltage and current values for all samples.

Building upon past research, table 3 delves into the performance of PENGs with as-fabricated ZnO nanorods, benchmarking them against previous studies on devices containing similar ZnO nanostructures.

Table 2: The values of the output voltage and current of both samples

Sample	Output voltage (mV)	Output current (µA)
ZnO thin film	0.18	10.58
ZnO nanorods	0.68	40

4. Conclusion

To summarize, our investigation provides a comparative assessment of ZnO nanostructures in one dimension (nanorods) and two dimensions (thin film), synthesized via the hydrothermal method and magnetron sputtering deposition, respectively. These findings carry significance for potential applications in energy harvesting or piezoelectric transduction. We conducted a thorough structural and morphological characterization, revealing the successful fabrication of high-quality the ZnO nanorods and the ZnO thin film on a flexible PET-ITO substrate.

Table 3. the characteristic parameters of recently reported piezoelectric nanogenerators (PENGs) alongside the results of this work

Sample	Substrate	Applied force (N)	Volatge/Current	Ref.
ZnO nanorods	Stainless-steel foils	6	2.6 (V)/-	[16]
ZnO nanorods	Textile cotton fabric	3×10^{-6}	9 (mV)/-	[17]
ZnO nanorods	Glass-ITO	-	56.3 (mV)/ 3.46 mA	[18]
ZnO nanorods	PET-ITO	10	26-28 mV/40 nA	[19]
ZnO nanosheets	PET-ITO	10	28-35 mV/ 150 nA	[19]
Patterned ZnO nanorods	PET-ITO	10	-/150 nA	[6]
This work	PET-ITO	2.6	0.65 mV/ 38 μA	This work

[Downloaded from azadandishi.iust.ac.ir on 2025-07-21]

[DOI: 10.22068/ase.2024.664]

Moreover, our study affirms that the PENG based on the ZnO nanorods demonstrated a substantial improvement in output voltage compared to the PENG relying on the ZnO thin film. The maximum output voltage, attributed to ZnO nanorods, measured approximately 0.68 mV, a value sufficient to power various nano/micro-electronic devices. These findings are poised to provide effective and valuable strategies for advancing highly energy-efficient ZnO nanogenerators and expanding the scope of nanogenerator applications in automotive industry, including energy harvesting from vehicle vibrations, self-powered sensors, smart interior features, vehicle health monitoring and energy-efficient lighting systems.

5. Reference

[1] C. Wei and X. Jing, "A comprehensive review on vibration energy harvesting: Modelling and realization," *Renew. Sustain. Energy Rev.*, vol. 74, pp. 1–18, 2017.

[2] J. Briscoe and S. Dunn, "Piezoelectric nanogenerators – a review of nanostructured piezoelectric energy harvesters," *Nano Energy*, vol. 14, pp. 15–29, 2015.

[3] J. Pei, F. Guo, J. Zhang, B. Zhou, Y. Bi, and R. Li, "Review and analysis of energy harvesting technologies in roadway transportation," *J. Clean. Prod.*, vol. 288, p. 125338, 2021.

[4] S. M. Hosseini, M. Soleymani, S. Kelouwani, and A. A. Amamou, "Energy Recovery and Energy Harvesting in Electric and Fuel Cell Vehicles, a Review of Recent Advances," *IEEE Access*, vol. 11, pp. 83107–83135, 2023.

[5] A. E. Akin-Ponnle and N. B. Carvalho, "Energy harvesting mechanisms in a smart city—a review," *Smart Cities*, vol. 4, no. 2, pp. 476–498, 2021.

[6] D. Yang *et al.*, "Patterned growth of ZnO nanowires on flexible substrates for enhanced performance of flexible piezoelectric nanogenerators," *Appl. Phys. Lett.*, vol. 110, no. 6, 2017.

[7] C. Pan, J. Zhai, and Z. L. Wang, "Piezotronics and Piezo-phototronics of Third Generation Semiconductor Nanowires," *Chem. Rev.*, vol. 119, no. 15, pp. 9303–9359, 2019.

[8] A. A. Semenova *et al.*, "Formation of ZnO nanorods on seed layers for piezoelectric nanogenerators," *J. Phys. Conf. Ser.*, vol. 917, no. 3, pp. 1–7, 2017.

[9] G. N. Narayanan, S. G. R, and A. Karthigeyan, "Effect of annealing temperature on structural, optical and electrical properties of hydrothermal assisted Zinc Oxide Nanorods," *Thin Solid Films*, p. 7, 2015.

[10] T. H. Flemban *et al.*, "A Photodetector Based on p-Si/n-ZnO Nanotube Heterojunctions with High Ultraviolet Responsivity," *ACS Appl. Mater. Interfaces*, vol. 9, no. 42, pp. 37120–37127, 2017.

[11] A. H. Farha, M. M. Ibrahim, and S. A. Mansour, "Ga-doped ZnO nanostructured powder for cool-nanopigment in environment applications," *Materials (Basel).*, vol. 13, no. 22, pp. 1–16, 2020.

[12] S. Rafique, A. K. Kasi, J. K. Kasi, Aminullah, M. Bokhari, and Z. Shakoor, "Fabrication of silver-doped zinc oxide nanorods piezoelectric nanogenerator on cotton fabric to utilize and optimize the charging system," *Nanomater. Nanotechnol.*, vol. 10, p. 1847980419895741, 2020.

[13] K. Khun, Z. H. Ibupoto, M. S. AlSalhi, M. Atif, A. A. Ansari, and M. Willander, "Fabrication of well-aligned ZnO nanorods using a composite seed layer of ZnO nanoparticles and chitosan polymer," *Materials (Basel).*, vol. 6, no. 10, pp. 4361–4374, 2013.

[14] R. S. Kammel and R. S. Sabry, "Effects of the aspect ratio of ZnO nanorods on the performance of piezoelectric nanogenerators," *J. Sci. Adv. Mater. Devices*, vol. 4, no. 3, pp. 420–424, 2019.

[15] A. T. Le, M. Ahmadipour, and S. Y.

[Downloaded from azadandishi.iust.ac.ir on 2025-07-21]

[DOI: 10.22068/ase.2024.664]

Pung, “A review on ZnO-based piezoelectric nanogenerators: Synthesis, characterization techniques, performance enhancement and applications,” *J. Alloys Compd.*, vol. 844, p. 156172, 2020.

[16] N. Mufti, A. Damayanti, Aripriharta, Arramel, A. Taufiq, and Sunaryono, “The Growth of ZnO Nanorods on Stainless-steel foils and Its Application for Piezoelectric Nanogenerator,” *J. Phys. Conf. Ser.*, vol. 1093, no. 1, 2018.

[17] A. Khan, A. Abbasi, M. Hussain, and Z. H. Ibupoto, “fabric Piezoelectric nanogenerator based on zinc oxide nanorods grown on textile cotton fabric,” vol. 193506, no. 2012, 2014.

[18] C. C. Chen *et al.*, “ZnO nanogenerator prepared from ZnO nanorods grown by hydrothermal method,” *Sensors Mater.*, vol. 31, no. 3, pp. 1083–1089, 2019.

[19] Q. Wang, D. Yang, Y. Qiu, X. Zhang, W. Song, and L. Hu, “Two-dimensional ZnO nanosheets grown on flexible ITO-PET substrate for self-powered energy-harvesting nanodevices,” *Appl. Phys. Lett.*, vol. 112, no. 6, 2018.

[Downloaded from azadandishi.iust.ac.ir on 2025-07-21]

[DOI: 10.22068/ase.2024.664]